Design and Geometric Transformations of Koch Curve Monopole Antennas

Atif Jamil
Department of Computer Systems Engineering
Dawood University of Engineering & Technology
Karachi, Pakistan
atif.jamil@duet.edu.pk

Khalid Rafique
Azad Jammu and Kashmir Information Technology Board
Azad Jammu & Kashmir, Pakistan
khalidrafiquepk@gmail.com

Muhammad Dawood Idrees
Department of Industrial Engineering and Management
Dawood University of Engineering & Technology
Karachi, Pakistan
muhammad.dawood@duet.edu.pk

Abdul Sami Rajput
Department of Electronic Engineering
Dawood University of Engineering & Technology
Karachi, Pakistan
dr.abdulsami@duet.edu.pk

Arif Abdullah
Department of Electronic Engineering
Dawood University of Engineering & Technology
Karachi, Pakistan
arif.abdullah@duet.edu.pk

Abdul Sattar Saand
Department of Electrical Engineering
Quaid-e-Awam University of Engineering, Science and Technology, Nawabshah, Pakistan
as-saand@quest.edu.pk

Received: 19 January 2022 | Revised: 1 March 2022 | Accepted: 9 March 2022

Abstract-In this paper, a modified Koch curve monopole antenna is proposed for the dual-band Wireless Local Area Network (WLAN) and its performance has been compared with the conventional printed Koch-curve monopole antenna. Both the antennas have been contrived, and their simulated return loss and radiation pattern results have been validated with the measurements. Antenna #1 is designed on the geometrical basis of a conventional Koch-curve monopole antenna. Moreover, the shape of antenna # 1 is bent with a two-step rotation process to yield antenna #2. There are two advantages to this geometrical modification: Firstly, the unique rotation in antenna #2 has further increased the mutual coupling between the segments of the Koch-curve geometry, and thus improved the impedance matching. Secondly, due to its geometric configuration that enhanced its ground plane size, the proposed antenna #2 has been able to demonstrate consistent simulation and measurement results. The compact ground plane in antenna #1 has been identified as the primary reason for the disagreement between the simulated and measured return loss results. The presented antennas have also been studied for the variation of indentation angles: θ=30 and θ=60.

Keywords-fractal antennas; multiband; geometry; Koch monopole; omnidirectional

I. INTRODUCTION

The size of the microstrip patch antennas has reduced to a large extent to suit the needs of modern wireless communications requirements. The antenna designers have expanded their horizons to design ultra-portable and multiband antennas, so that they may fit into the chassis of the compact hand-held wireless communication terminals. Moreover, the challenge of size reduction has a trade-off with the antenna bandwidth and efficiency [1]. A good antenna design cycle has an emphasis on the optimization of many performance parameters. Some of the commonly strived parameters in a good antenna design include frequency tuning, impedance matching, high gain, and better radiation characteristics in the desired bands. Many of these antenna parameters are optimized during simulations.

Fractals have been defined as the geometry possessing the properties of self-similarity. The fractal geometry is nowhere distinguishable at any scale of magnification. The scaled up or scaled down versions of fractal geometry are exactly identical to the original (non-scaled) versions. The fundamental limit on the antenna size has been demonstrated in [1]. The behavior of the Koch curve monopole antenna has been discussed, and its relation to the fundamental limit of the small antennas has been presented in [2]. Many authors have investigated the behavior of the applied geometrical transformations on Koch-curve antenna and its effect on performance parameters [3, 4]. There is some degree of freedom with which one can design Koch-curve monopoles. The Koch monopole can be bent in particular ways to extend the current path through geometry while shrinking the antenna dimensions. The geometry of the Koch-curve monopole antennas can yield the same area as Euclidean

Corresponding author: Atif Jamil

antennas, but the current has an extended path. Higher Fractal iterations are applied to lower the frequency [5]. However, with the increasing fractal iterations, the overall size of the antenna also increases [6]. It is a well-known fact that the antenna size should be an appropriate fraction of the wavelength. When the antenna size is decreased more than the operating wavelength, the efficiency of the antenna decreases significantly. Unlike the Euclidean geometries, the occurrences of the multi-band behavior of the fractal antennas are not related to the electrical length, they are rather related to the geometry and the log periodic behavior of the antennas. Many fractal geometries have been used in antenna designs, and the relation between the variation of geometrical angles and antenna's performance characteristics has been presented in [7]. Such studies show that the change of indentation angle directly affects the input resistance and occurrence of the resonant frequencies. The log periodic behavior of the fractal antennas has been attributed to the factor, by which their geometries are scaled [8, 9]. In fractal antennas, the ratio of the first two resonant frequencies can be controlled by the ratio of the antenna dimensions. Many dimensional ratios of the overall radiating structure, including ground plane dimensional ratios and other geometrical variations can change this ratio. In [10], the authors controlled the ratio of the first two frequencies by changing *h*/*w*. A compact single probe feed asymmetrical semicircular fractal boundary patch antenna based on HIS (High Impedance Surface) is proposed for wide bandwidth at the Wi-Fi band in [11]. A fractal antenna array for telecommunication applications is presented in [12].

Many studies have investigated the measurement-related problems, posed by the Electrically Small Antennas (ESAs). Here, we will limit the scope of the study to the measurement issues related to the small, convoluted shaped antennas. The stringent requirement on the size reduction of modern day antennas has also reduced their ground plane size. The ground plane size in small antennas plays an active role in radiation. Certain parameters are affected by the small ground plane size, including a shift in resonant frequencies, impedance mismatch, impedance bandwidth, low gain, low efficiency, and distorted radiation patterns [13, 14]. The effect of the ground plane is also crucial in the design of monopole antennas [15].

This paper presents the results and a discussion on the issues pertinent to the measurement of small antennas, particularly with a small ground plane. The performances of the two designed and developed Koch-monopole antennas were compared by the simulation and measurement results. A parametric study has been carried out in order to study the effects of changing the geometrical indentation angles on the shift in resonant frequencies. Moreover, a study on the surface current distribution is presented to understand the multiband behavior of both antennas.

II. ANTENNA GEOMETRIC CONFIGURATION

In this section, two geometric configurations have been realized with two different indentation angles. The indentation angle is an essential element in determining the length of the adjacent segment. The construction of the two antennas is based on iterative transformation. The Iteration Function System (IFS) [16] offers an integrated platform for the development of Fractal geometries including Koch curves. In the plane $\omega : R^2 \to R^2$, the affine transformations are defined as in (1):

$$\omega\begin{pmatrix} x_1 \\ x_2 \end{pmatrix} = \begin{pmatrix} a & b \\ c & d \end{pmatrix}\begin{pmatrix} x_1 \\ x_2 \end{pmatrix} + \begin{pmatrix} \mathrm{e} \\ f \end{pmatrix} = Ax + t \quad (1)$$

Equation (1) can also be described as:

$$\omega(x, y) = (ax_1 + bx_2 + \mathrm{e}, cx_1 + dx_2 + f) \quad (2)$$

In (1), the matrix A can be defined as in (3) and the point x has the coordinates x_1 and x_2. The matrix t gives the translation on the plane. The parameters *a*, *b c*, *d*, control the rotation and scaling while the linear translation on the plane is controlled by the parameters *e* and *f*.

$$A = \begin{pmatrix} \delta\cos\theta & -\delta\sin\theta \\ \delta\sin\theta & \delta\cos\theta \end{pmatrix} \quad (3)$$

In (3), δ is the scaling factor, such that $0 \le \delta \le 1$ and θ is the rotation angle. The described geometries in this paper have been scaled by $1/3$. For the two cases analyzed in this paper, the angles of rotation are $\theta_1 = 30^\circ$ and $\theta_2 = 60^\circ$. In assumption, if $\omega_1, \omega_2, \omega_3 \ldots\ldots \omega_n$ are the set of affine transformations and if the initial geometry is given by A, a new geometry can be constructed by applying a set of transformations to $A(2)$. The collective results are expressed by (4).

$$W(A) = \bigcup_{n=1}^{N} \omega_n(A) \quad (4)$$

W is the Hutchinson operator which determines the looked-for iteration by the repeated application of W to the previous geometry such that if the initial geometry is A_0 then:

$$A_1 = W(\mathrm{A}_0)\ A_2 = W(\mathrm{A}_2)\ A_K = W(\mathrm{A}_{(K-1)}) \quad (5)$$

The method for determination of the geometric structure is to calculate the fractal dimension of a line as a function. Two measurement points are taken when associating the fractal with some discrete boxes. These boxes are vital for the calculation of a set of points in a plane.

$$N(\delta) = \delta^{-D} \quad (6)$$

In (6), the $N(\delta)$ is the number of the required boxes. The dimension of a box is defined in (6). Equation (6) can be written after taking the logarithm on both sides as in (7):

$$\log\left[N(\delta)\right] = -D\log(\delta) \quad (7)$$

$$D = \frac{\log\left[N(\delta)\right]}{\log 1/\delta} \quad (8)$$

In (8), the dimension D is the ratio of the newly formed element $N(\delta)$ to the inverse if scaling factor $1/\delta$.

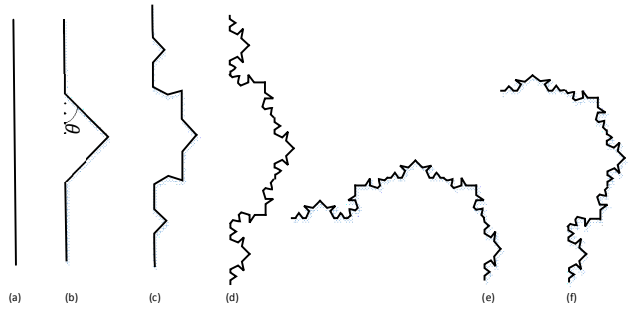

Fig. 1. Iterations of the Koch monopole antenna: (a) Straight strip, (b) first iteration, (c) second iteration, (d) third iteration, (e) modified Koch curve antenna, (f) finalized antenna design.

The construction procedure of the antenna #1 and antenna #2 with an indentation angle of $\theta = 30^0$ and $\theta = 60^0$ is illustrated in Figure 1(a)-(b). The design process of geometric transformation starts by taking into account the length of a straight strip of length h. The strip is divided into three equal parts, the middle section is replaced by an equilateral triangle of length $L/3$. For obtaining the first iteration which is depicted in Figure 1(b), (4) can be written as:

$$W(A) = \omega_1(A) \cup \omega_2(A) \cup \omega_3(A) \cup \omega_4(A) \quad (9)$$

The final Pattern in Figure 1 is obtained by a series of geometric transformations on the shape achieved in the first iteration. The antenna is then rotated by a two-step procedure to reduce its overall length. Here, we will focus on tuning the resonant frequencies with modifying indentation angles. The increase in indentation angles increases the length of the subsequent segments and in turn the space occupied by the Koch monopole antenna is also enhanced. In this way, the overall area occupied by the radiator is enlarged, and the resonant frequencies can be lowered. Figures 2-3 depict the comparison plots of the two indentation angles, $\theta = 30^0$ and $\theta = 60^0$ for antenna #1 and antenna #2 respectively. It can be noticed that with the decrease of the indentation angle of antenna #1, the input impedance at the resonant bands also changes, accounting for impedance mismatch [3]. With the decrease in indentation angle, similar changes can also be noticed in Figure 3. Here, the impedance mismatch is somehow better matched than the comparison plot of Figure 2. This is mainly due to the enhanced ground plane of the antenna #2. The discussion on the effects of the ground plane on antennas' performance and measurement results are presented in a separate section. In both antennas, the geometrical configuration with higher indentation angle, i.e. $\theta = 60^0$, along with the third iteration, lowered the resonant frequencies to the desired bands. The increase in indentation angles brought the inverted-V arm closer, increasing the capacitance between them. Hence, the mutual coupling between the Koch-curve member elements is enhanced. As the number of iterations increases, the proportional electrical length is also increased which in turn produces an additional equivalent inductance [7].

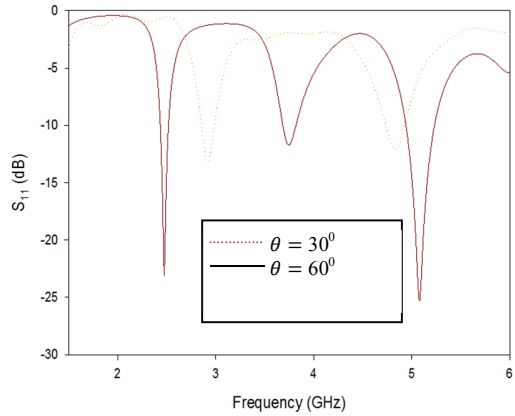

Fig. 2. Antenna #1: Effect of the variation of indentation angle on the resonant frequency.

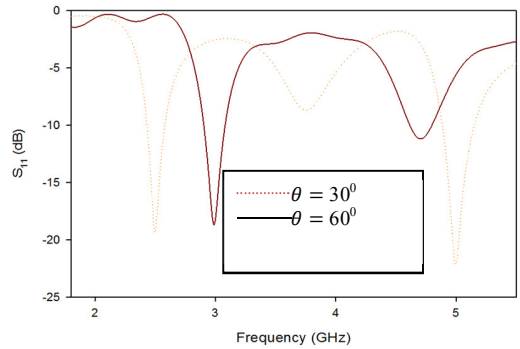

Fig. 3. Antenna #2: Effect of the variation of indentation angle on the resonant frequency.

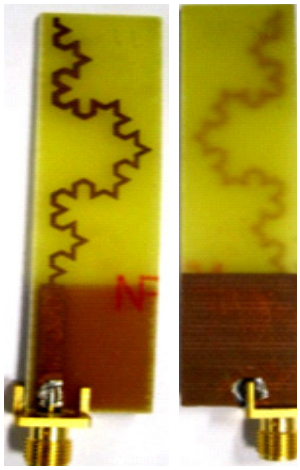

Fig. 4. Photograph of fabricated antenna #1 on substrate (a) top view, (b) bottom view.

III. ANTENNA DIMENSIONS

The detailed dimensions of the antennas are presented in Table I. The parametric study on the role of indentation angles has been carried out through the simulations. All the four geometrical configurations have been simulated. Due to the involved cost factor, only the antennas which yielded the optimal results, i.e. antenna #1 and antenna #2 with an

indentation angle of $\theta = 60^0$ were fabricated on FR-4 substrate and were compared with the correspondent simulation results. It can be noticed from Table I that the overall dimensions including the ground plane dimensions of antennas #1 and #2 with indentation angles of $\theta = 30^0$ and 60^0 are similar. However, due to an increase in the indentation angle, patch dimensions have been enhanced in the third and fourth column of Table I.

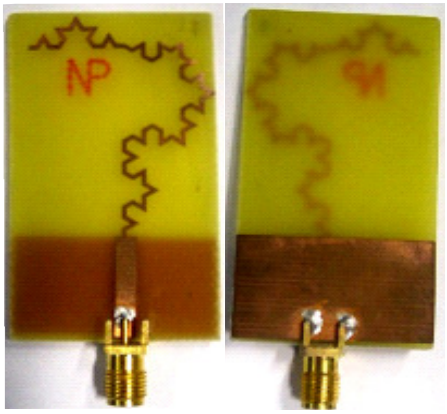

Fig. 5. Photograph of fabricated antenna #2 on substrate (a) top view, (b) bottom view.

TABLE I. VARIOUS CONFIGURATIONS' ANTENNA DIMENSIONS

Configurations	**Antenna #1 $\theta = 30^0$**	**Antenna #2 $\theta = 30^0$**	**Antenna #1 $\theta = 60^0$**	**Antenna #2 $\theta = 60^0$**
Overall dimensions (mm^3)	73×16×1.6	55×30×1.6	73×16×1.6	55×30×1.6
Patch dimensions (mm^2)	49×10.8	37×16.7	49×13	37×28
Ground plane dimensions (mm^2)	23×16	16×30	23×16	16×30
Thickness of copper (μm)	35	35	35	35
Dielectric constant	4.34	4.34	4.34	4.34

Further discussion in the subsequent sections concentrates mainly on understanding the multiband behavior of the two antennas and the cable effects on the small ground plane size during measurements. It does not include the discussion of the indentation angles. For the mentioned reason we have discarded the antennas with an indentation angle of $\theta = 30^0$ from the mentioned investigations.

IV. CURRENT DISTRIBUTION

For studying the multiband behavior of the Koch monopole antenna, it is necessary to determine the surface current distribution on the antenna segments. The current allocation of these segments handles radiation from the antenna at any specific frequency. Figure 6 depicts the surface current distribution on the surface of antennas #1 and #2. Both antennas are placed on the top layer, and the ground plane is located at the bottom layer. The surface current distribution on antenna #1 at 2.45 and 5GHz can be seen in Figure 6(a) and 6(b) respectively. Figures 6(c) and (d) depict the active segments responsible for radiation from antenna #2 at 2.45 and 5GHz. It is noticed that the radiation on 2.45GHz from antenna #1 is mainly due to the concentration of the surface current vectors in the lower part of the antenna. The radiation at 5GHz from antenna #1 is due to the surface current distribution on the upper and lower sections of the antenna, as illustrated in Figure 6(b). The surface currents depicted in Figure 6(c) show the $\lambda/4$ operation of antenna #2 at 2.45GHz. The operation of antenna #2 on 5GHz is due to the random distribution of surface current vectors on the entire structure, with nulls in between. The ground plane also has a vital role in the construction of small antennas. Through current excitation, a monopole antenna ground plane creates another half of the monopole, so that it can act as a dipole antenna. The ground plane plays an active part in the radiation mechanism of small antennas. In this study, the ground plane effect on the performance of both antenna structures is significantly noticed as the height of the ground plane influences the shift in resonant frequencies on both antennas. The excitation of current in both antennas is introduced by a transmission line through a 50Ω excitation port. Through simulations, the position of placement for both antennas on the ground plane is optimized for achieving good impedance match that results in reduced return loss.

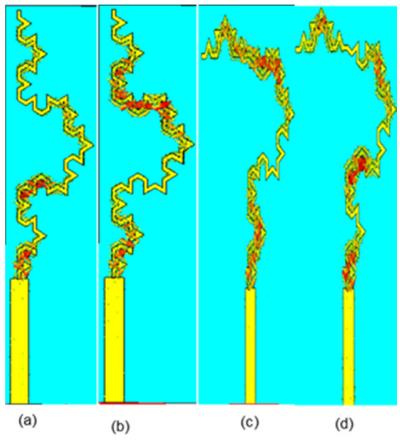

Fig. 6. Current distribution on antenna #1 at (a) 2.45GHz, (b) 5GHz. Surface current on antenna #2 at (c) 2.45GHz, (d) 5GHz.

V. EFFECTS OF THE GROUND PLANE ON MEASUREMENT RESULTS

Both antennas presented in this paper portray good agreement between the simulation and the measurement results. The study presented in this section is primarily an investigation on the ground plane size. The experimental study of antenna #1 showed that the compact and insufficient ground plane is the prime hindrance in achieving measurement results similar to the simulation results. The measurements were carried out on Agilent E8363C PNA network analyzer. The measurement setup of the PNA is matted with a coaxial cable. In small and unbalanced antennas, the cable currents mainly reside on the outer conductor of the cable [11]. The remedy to subside this large current on the outer conductor of the cable is to increase the width of the ground plane, and so the current distributes on it. In antenna #1, due to the geometrical limitations, the ground plane size is limited. In the case of

antenna #2, the width of the ground plane was automatically increased as we bend the geometry of Koch-monopole antenna. The larger ground plane yielded better measurement result and more comparable with the simulation. Realistically, in robust conditions, the antenna measurement is affected by some factors such as coupling with cables, connectors, and fabrication tolerances. The discussion on the ground plane effects is meant to provide insight into the understanding of these factors during measurements.

VI. RESULTS AND DISCUSSION

It can be noticed from the curves presented in Figures 7-8, that both antennas have satisfactory return loss results. The antennas are designed to operate on the WLAN frequency bands of 2.45 and 5GHz. The measured S11 plot of antenna #1 shows an impedance bandwidth of 153MHz at -10dB scale, around the center frequency of 2.496GHz and a bandwidth of 232MHz around the center frequency of 5.02GHz. For the antenna #2, the measured bandwidth calculated at -10dB scale for the 2.45GHz band is 180MHz. The antenna #2 depicts satisfactory return loss measurement performance at the 5GHz band, with a minimum return loss of -24.4dB at 4.97 GHz and the calculated impedance bandwidth is 285MHz. The far-field performance of the antennas #1 and #2 has been gauged by the measurement of the E-plane and H-plane patterns at 2.45GHz and 5GHz. The patterns for antenna #1 are presented in Figures 9 and 10.

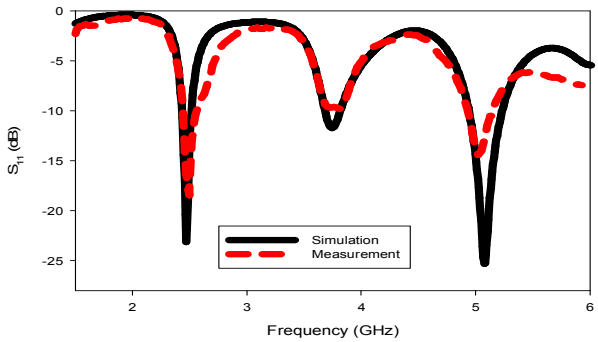

Fig. 7. Antenna# 1: Comparison between simulation and measurement S11 results.

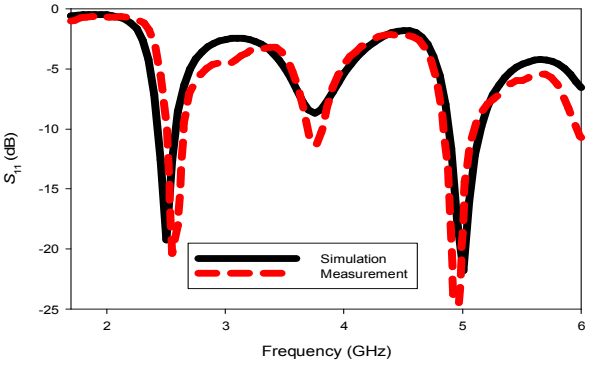

Fig. 8. Antenna #2: Comparison between simulation and measurement S11 results.

Figures 11 and 12 show the radiation patterns of the antenna #2. The shape of the plots is mostly symmetric in both E and H fields. In the case of antenna #1, it has been observed that the radiation pattern plot is omnidirectional at 2.45GHz and 5GHz with gains of 4.15dBi at 2.45GHz and 2.57dBi at 5GHz. The far-field radiation pattern of antenna #2 at 2.45GHz depicts that the antenna demonstrates a good omnidirectional H-plane pattern while exhibiting a figure-eight pattern in the E-plane. It can be seen from Figure 12 that the radiation pattern of antenna #2 has been distorted in E and H planes. Due to the bending of antenna #2, this distortion has caused an alteration in current distribution on the antenna structure. The horizontal component of the electric field in antenna #2 is mainly concentrated on the upper and lower sections of the antenna. The horizontal component of the electric field causes a distortion of the radiation pattern at a higher resonant frequency of 5GHz. The simulated directivity gains along the X-Y plane are 1.3dBi at 2.45GHz and 4.2dBi at 4.93GHz.

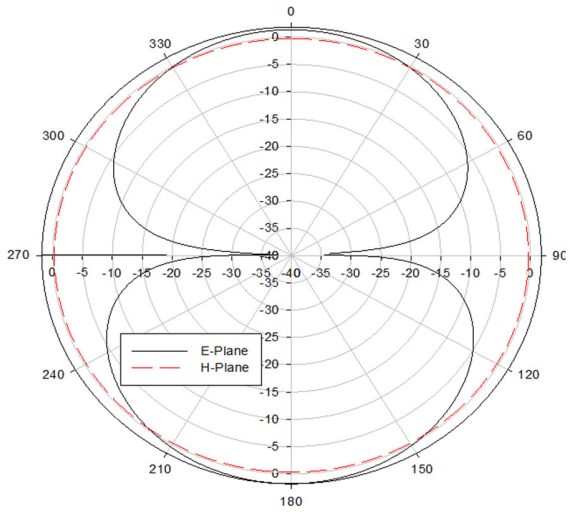

Fig. 9. Measured E-plane pattern of antenna #1 at 2.45 GHz.

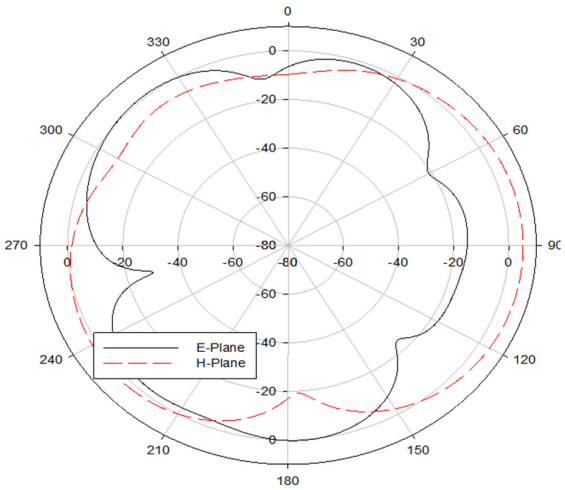

Fig. 10. Measured H-plane pattern of antenna #1 at 5GHz..

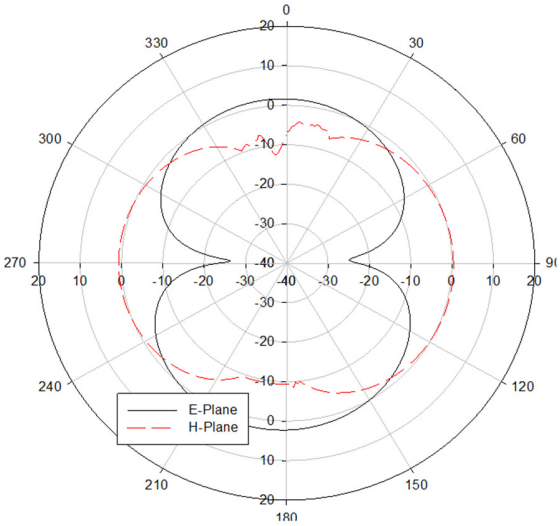

Fig. 11. Measured E-plane pattern of antenna #2 at 2.45GHz.

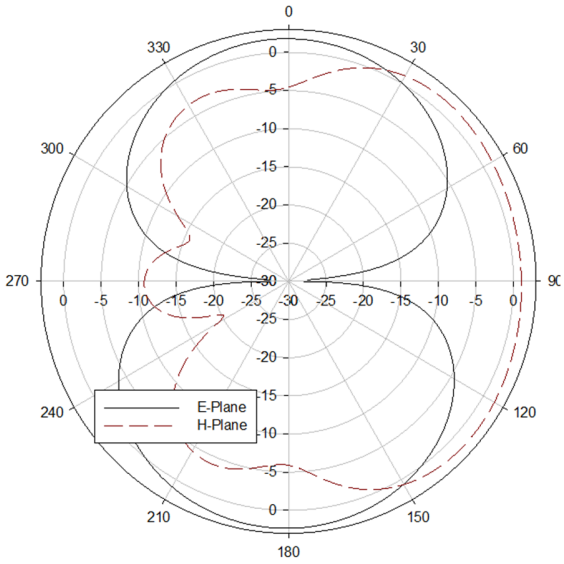

Fig. 12. Measured H-plane pattern of antenna #2 at 5GHz.

VII. CONCLUSION

In this paper, a technique has been proposed to reduce the size of the conventional Koch-curve monopole antenna along with a parametric study on the role of indentation angles. The higher indentation angle along with the higher number of iterations has a great impact on the novel space-filling property of the fractal antennas. Moreover, the proposed technique to reduce the antenna size also introduced an additional width to the ground plane of antenna #1. During the process of small antenna designs, most of the designs ignore the effects of the coaxial cable and the connector. Cable effects can become the primary reason for the discrepancy between the simulation and the measurement results beside other valid reasons such as fabrication, soldering and measurement tolerances. The increased ground plane width in antenna #2 portrayed better S11 measurement results. The measured E and H-plane radiation pattern results at the resonant frequency of 2.45GHz and 5GHz have been presented for both antennas. The omnidirectional radiation pattern results helped confirm that the designed fractal Koch-curves are monopole antennas.

REFERENCES

[1] L. J. Chu, "Physical Limitations of Omni-Directional Antennas," *Journal of Applied Physics*, vol. 19, no. 12, pp. 1163–1175, Dec. 1948, https://doi.org/10.1063/1.1715038.

[2] C. P. Baliarda, J. Romeu, and A. Cardama, "The Koch monopole: a small fractal antenna," *IEEE Transactions on Antennas and Propagation*, vol. 48, no. 11, pp. 1773–1781, Aug. 2000, https://doi.org/10.1109/8.900236.

[3] C. Puente, J. Romeu, R. Pous, J. Ramis, and A. Hijazo, "Small but long Koch fractal monopole," *Electronics Letters*, vol. 34, no. 1, pp. 9–10, Jan. 1998, https://doi.org/10.1049/el:19980114.

[4] K. J. Vinoy, J. K. Abraham, and V. K. Varadan, "On the relationship between fractal dimension and the performance of multi-resonant dipole antennas using Koch curves," *IEEE Transactions on Antennas and Propagation*, vol. 51, no. 9, pp. 2296–2303, Sep. 2003, https://doi.org/10.1109/TAP.2003.816352.

[5] S. R. Best, "On the performance properties of the Koch fractal and other bent wire monopoles," *IEEE Transactions on Antennas and Propagation*, vol. 51, no. 6, pp. 1292–1300, Jun. 2003, https://doi.org/10.1109/TAP.2003.812257.

[6] S. Zainud-Deen, H. A. E.-A. Malhat, and and K. Awadalla, "Fractal Antenna for Passive UHF RFID Applications," *Progress In Electromagnetics Research B*, vol. 16, pp. 209–228, 2009, https://doi.org/10.2528/PIERB09051506.

[7] R. Ghatak, D. R. Poddar, and R. K. Mishra, "A moment-method characterization of V-Koch fractal dipole antennas," *AEU - International Journal of Electronics and Communications*, vol. 63, no. 4, pp. 279–286, Apr. 2009, https://doi.org/10.1016/j.aeue.2008.01.010.

[8] C. P. Baliarda, C. B. Borau, M. N. Rodero, and J. R. Robert, "An iterative model for fractal antennas: application to the Sierpinski gasket antenna," *IEEE Transactions on Antennas and Propagation*, vol. 48, no. 5, pp. 713–719, Feb. 2000, https://doi.org/10.1109/8.855489.

[9] C. T. P. Song, P. S. Hall, H. Ghafouri-Shiraz, and I. Henning, "Fractal antenna research at University of Birmingham," in *2001 Eleventh International Conference on Antennas and Propagation, (IEE Conf. Publ. No. 480)*, Manchester, UK, Apr. 2001, vol. 2, pp. 724–727, https://doi.org/10.1049/cp:20010386.

[10] P. Hazdra, J. Eichler, M. Capek, P. Hamouz, and T. Korinek, "Small dual-band fractal antenna with orthogonal polarizations," in *Proceedings of the 5th European Conference on Antennas and Propagation (EUCAP)*, Rome, Italy, Apr. 2011, pp. 2733–2736.

[11] S. Nelaturi and N. V. S. N. Sarma, "Compact Wideband Microstrip Patch Antenna based on High Impedance Surface," *Engineering, Technology & Applied Science Research*, vol. 8, no. 4, pp. 3149–3152, Aug. 2018, https://doi.org/10.48084/etasr.1971.

[12] C. B. Nsir, J. M. Ribero, C. Boussetta, and A. Gharsallah, "Design of a 1×2 CPW Fractal Antenna Array on Plexiglas Substrate with Defected Ground Plane for Telecommunication Applications," *Engineering, Technology & Applied Science Research*, vol. 11, no. 6, pp. 7897–7903, Dec. 2021, https://doi.org/10.48084/etasr.4558.

[13] M. V. Rusu and R. Baican, "Microwave and Millimeter Wave Technologies," in *Fractal Antenna Applications*, I. Minin, Ed. IntechOpen, 2010, https://doi.org/10.5772/9057.

[14] I. T. Nassar and T. M. Weller, "The ground plane effect of a small meandered line antenna," in *WAMICON 2011 Conference Proceedings*, Clearwater Beach, FL, USA, Apr. 2011, pp. 1–5, https://doi.org/10.1109/WAMICON.2011.5872862.

[15] H. Alsaif, "Compact Hexagonal Monopole Antenna for Lower 5G Bands," *Engineering, Technology & Applied Science Research*, vol. 9, no. 3, pp. 4200–4202, Jun. 2019, https://doi.org/10.48084/etasr.2714.

[16] J. P. Gianvittorio and Y. Rahmat-Samii, "Fractal antennas: a novel antenna miniaturization technique, and applications," *IEEE Antennas and Propagation Magazine*, vol. 44, no. 1, pp. 20–36, Oct. 2002, https://doi.org/10.1109/74.997888.